LIMNOLOGY
and
OCEANOGRAPHY

ASLO

Limnol. Oceanogr. 00, 2015, 00–00

doi: 10.1002/lno.10212

Bacterial and protist community changes during a phytoplankton bloom

John K. Pearman,*[1] Laura Casas,[1] Tony Merle,[†2] Craig Michell,[1] Xabier Irigoien[1]

[1]Biological and Environmental Science and Engineering Division (BESE), Red Sea Research Center, KAUST-King Abdullah University of Science and Technology, Thuwal, Saudi Arabia

[2]Biological and Environmental Science and Engineering Division (BESE), Water Desalination and Reuse Center, KAUST-King Abdullah University of Science and Technology, Thuwal, Saudi Arabia

Abstract

The present study aims to characterize the change in the composition and structure of the bacterial and microzooplankton planktonic communities in relation to the phytoplankton community composition during a bloom. High-throughput amplicon sequencing of regions of the 16S and 18S rRNA gene was undertaken on samples collected during a 20 day (d) mesocosm experiment incorporating two different nutrient addition treatments [Nitrate and Phosphate (NPc) and Nitrate, Phosphate and Silicate (NPSc)] as well as a control. This approach allowed us to discriminate the changes in species composition across a broad range of phylogenetic groups using a common taxonomic level. Diatoms dominated the bloom in the NPSc treatment while dinoflagellates were the dominant phytoplankton in the control and NPc treatment. Network correlations highlighted significant interactions between OTUs within each treatment including changes in the composition of Paraphysomonas OTUs when the dominant *Chaetoceros* OTU switched. The microzooplankton community composition responded to changes in the phytoplankton composition while the prokaryotic community responded more to changes in ammonia concentration.

In marine ecosystems phytoplankton capture energy from sunlight and transforms it into organic material (biomass) that feeds planktonic foodwebs. Transient increases in the abundance of phytoplankton and the domination of one or a few species are referred to as blooms. In general there is a positive correlation between the abundance of phytoplankton cells and heterotrophic bacteria, with a large proportion of the organic matter present during a bloom being recycled via bacteria (Cole et al. 1988; Ducklow et al. 1993). Organic matter not recycled by bacteria in the microbial loop (Azam et al. 1983) can be transferred to higher trophic levels through primary consumers such as protists (Sherr and Sherr 2002) and zooplankton (Irigoien et al. 2000) or transported to the deep ocean either via the biological pump (Longhurst and Harris 1989) or direct sinking (Billet et al. 1983).

The fate of the biomass produced by the bloom depends not only on the phytoplankton community but also on the community of the heterotrophic consumers (bacteria and zooplankton) and the ability to feed on the species dominating the bloom. Both bacterioplankton and zooplankton biomass are coupled to phytoplankton biomass (Moran et al. 2002; Irigoien et al. 2004) with a time lapse that depends on life cycle and temperature (Rose and Caron 2007). However, the extent to which the phytoplankton bloom species affects the composition of the bacteria and zooplankton community is not well known. Bacterioplankton and microzooplankton have been shown to exhibit changes in composition during the blooms (Riemann et al. 2000; Pinhassi and Berman 2003; Rink et al. 2007; Löder et al. 2011; Teeling et al. 2012; Buchan et al. 2014) but it is often difficult to separate the effect of an increase in available food from changes in the phytoplankton composition. Bacterioplankton studies, undertaken in laboratory microcosms, suggest that there are differences in the bacterial community dependent on the phytoplankton bloom species (Pinhassi et al. 2004; Grossart et al. 2005).

In terrestrial ecosystems it is common to find a relation between the biodiversity of plants and herbivores. Conversely, in marine ecosystems the relation between phytoplankton and herbivore biodiversity is a subject of debate.

Additional Supporting Information may be found in the online version of this article.

[†]Present address: Department of Water Resources and Drinking Water, Eawag - Swiss Federal Institute of Aquatic Science and Technology, Dübendorf, Switzerland

*Correspondence: john.pearman@kaust.edu.sa

Using a large scale dataset Irigoien et al. (2004) found no relation between microzooplankton and phytoplankton biodiversity. However Dolan (2005) argued that the lack of relation could be mostly due to the different resolution in taxonomic determination for phytoplankton and microzooplankton in the database. Actually taxonomic determination is a real problem when studying biodiversity relationships between different groups of bacteria and protists because the degree of taxonomic determination using morphology is size dependent (i.e., small cells do not present morphological differentiations) and therefore different sizes are often identified at different taxonomic levels. However, the use of molecular tools has opened the way to study biodiversity with a coherent approach across different groups (Caron et al. 2004).

The objective of this study was to investigate to what extent bacteria and microzooplankton community composition respond to changes in phytoplankton species composition during a bloom. With that objective in mind we conducted a mesocosm experiment where we stimulated blooms of diatoms and dinoflagellates using different enrichments and followed the evolution of whole community diversity using molecular tools (16S and 18S amplicon sequencing).

Methods

Experimental design

A total of six mesocosm bags of 8000 L (depth: 2.5 m) were situated in the harbor of King Abdullah University of Science and Technology (KAUST), Thuwal, Saudi Arabia (Lat: 22.304°N Long: 39.103°E). Sampling took place over 20 d between the 27th January and the 15th February 2013. Nitrate ($NaNO_3$), phosphate ($H_2NaO_4P.H_2O$) and silicate ($Na_2SiO_3{\cdot}9H_2O$) were added into the mesocosm bags, which had been filled with harbor water, with three different treatments and two replicates per treatment: (1) a continuous addition of nitrate and phosphate (NPc) for the first 2 weeks, (2) a continuous addition of nitrate, phosphate and silicate (NPSc) for the first 2 weeks and (3) controls without nutrients addition. In this study, continuous addition is the addition of nutrients everyday at 6 am for the first 2 weeks. The nutrient concentrations added daily were Nitrate = 2 μM, Phosphate = 0.12 μM, Silicate = 3.75 μM adapted from the ratios published by Wyman et al. (2000). The concentrations used were tested in a small-scale microcosm experiment to show that the concentrations were able to induce a phytoplankton bloom (based on microscopic cell counts).

Sample collection

Temperature, salinity, and fluorescence profiles were measured daily using a CTD (Valeport Monitor CTD Profiler with an attached chlorophyll sensor).

A total of 20 L of water was collected from each mesocosm, at a depth of 1 m. Samples were taken at solar noon each day using a Niskin bottle. Water samples were immediately transferred to carboys for immediate filtration.

Samples were filtered using peristaltic pumps at low speed (70 rpm) to avoid destruction of delicate cells. Approximately 4 L of seawater was filtered through a 0.2 μm CellTrap^{TM} (Mem-Teq, U.K.). Concentrated cells were eluted from the CellTrap^{TM} using 2 mL of filtered seawater (from the same sample). Samples were immediately frozen in liquid nitrogen and stored at −80°C for later analysis.

Algae communities were quantified with a FACSVerse flow cytometer (Becton Dickinson, Belgium). 15 mL of water were collected and filtered through a 40 μm mesh. Samples were fixed in gluteraldehyde (2.5% final conc.) and immediately flash frozen in liquid nitrogen. Cells were excited with a blue laser at a wavelength of 488 nm and red fluorescence emissions were measured to discriminate picoeukaryotic and nanoeukaryotic phytoplankton. 1.002 μm beads (Polysciences, Europe) were added to each sample for verification of the equipment.

Samples for nutrients were collected based on the procedures described by Brügmann and Kremling (2007) and Kremling and Brügmann (2007). Briefly, water samples were filtered through a 0.45 μm filter into acid washed (10% HCl overnight) sample bottles and stored at −20°C for later analysis. Nitrate, nitrite, and orthophosphate were analyzed by means of an Autoanalyser AAIII pentacanal BRAN-LUEBBE (with 10 nm optical path) following the methods of Grasshoff et al. (1983) at AZTI Tecnalia. Ammonia was analyzed by a SEAL Analytical AutoAnalyzer 3 at KAUST using the protocols of the manufacturer.

DNA extraction and PCR amplification

Cells were pelleted via centrifugation (21,000 × g for 15 min at 4°C) and the supernatant was removed. Cells were resuspended in 180 μL ATL buffer (Qiagen) and 20 μL lysozyme (20 mg/mL) for 30 min at 37°C. Approximately 15 mg of 0.1 mm Zirconia/Silica Beads were added and cells were lysed using a Tissue LyserII machine (Qiagen) for 1 min at maximum speed (30 Hz). Proteinase K (20 μL at 20 mg/mL) and 5 μL RNAse (100 mg/mL) were added to the solution and incubated at 56°C overnight to ensure complete lysis. Following lysis an equal volume of phenol: chloroform: isoamyl alcohol (IAA) (25 : 24 : 1) was added, mixed gently for 5 min and centrifuged for 10 min at 10,000 × g. The aqueous layer containing the DNA was transferred into a new tube and an equal volume of phenol: chloroform: IAA was added. A third round with phenol: chloroform: IAA was performed. The aqueous layer was again transferred into a new tube and an equal volume of chloroform: IAA (24: 1) was added, mixed for 2 min and centrifuged for 5 min at 21,000 × g. DNA was precipitated by adding 2. vol. ethanol and 0.1 vol. sodium acetate (3 M, pH 5.2) and incubated at −20°C, pelleted, washed in 70% ethanol and then resuspended in 10–30 μL DNAse free water.

Amplification of the V9 region of the eukaryotic small subunit 18S rRNA gene used the 1389F/1510R primer set (Amaral-Zettler et al. 2009). PCR amplicons were generated for each sample in duplicate 50 μL reaction volumes. The

PCR conditions for the 18S rRNA gene were adapted from those described in Amaral-Zettler et al. (2009). An initial denaturation step of 3 min at 94°C was followed by 30 cycles of 94°C for 30 s, 57°C for 45 s and 72°C for 45 s. This is followed by a final extension at 72°C for 10 min.

Bacterial amplicons were produced by targeting the 16S V3 and V4 regions (Klindworth et al. 2013). Illumina adapter overhang nucleotide sequences were added to the gene specific sequences (see Supporting Information Table S1 for primer sequences). The PCR conditions for the 16S rRNA gene were adapted from those described in Klindworth et al. (2013). An initial denaturation step of 3 min at 95°C was followed by 25 cycles of 95°C for 30 s, 55°C for 30 s and 72°C for 30 s. This is followed by a final extension at 72°C for 5 min. Each reaction contained 2.5 U Taq (Invitrogen), 1X reaction buffer, 200 μM dNTPs, (Invitrogen), 2 mM $MgSO_4$ and 0.05 mg Bovine Serum Albumin (BSA). A total of 0.2 μM of both forward and reverse primer were added to the PCR mixture. A negative no template control was run for each primer pair.

Duplicate PCRs reactions from each sample were merged before PCR clean up. The 18S rRNA gene amplicon products were excised from a 1% agarose gel and purified using Qiagen's gel extraction kit while the 16S rRNA gene amplicons were cleaned up using Sequalprep normalization kit (Life Technologies). 18S rRNA gene samples with unique barcodes were pooled together (to a maximum of 15 samples per pool) and the presence of contaminating primer dimers was assessed by an Agilent 2100 bioanalyzer. The nuclear 18S rRNA gene amplicons were sequenced by Macrogen (Korea). Emulsion PCR was undertaken using Roche's protocols and each pooled sample was sequenced on a 1/4 of a run on a Roche 454 GS FLX machine. The purified 16S amplicons underwent a second round of PCR to attach dual indices using the Nextera XT index kit following the kits protocols. Indexed amplicons were purified using the Sequalprep normalization kit and pooled together (max 96 samples per pool). Samples were sequenced on a Illumina MiSeq at the King Abdullah University of Science and Technology sequencing core lab. Sequences were submitted to the NCBI Sequence Read Archive under experiment accession number: SRP051855.

Bioinformatic analysis

Amplicon sequences for both the 16S and 18S rRNA gene were analyzed using a QIIME (Caporaso et al. 2010) pipeline. Pooled 18S rRNA gene samples were demultiplexed based on barcodes. Raw reads were filtered based on quality ($q = 25$ over a window of 25) and length (minlength = 100, maxlength = 200). No ambiguities, a homopolymer length of 6 and 1 mismatch in the forward primer were allowed. Paired end 16S amplicon sequences were joined using the join_paired_ends.py script in QIIME and the resulting fastq file was quality filtered ($q = 20$) using split_libraries_fastq.py. Sequences were trimmed to the reverse primer. Filtered sequences were merged (16S and 18S separately) and pre-clustered using CDHIT (Li and Godzik 2006) and the trie setting (to remove subsequences of other sequences) before being clustered using USEARCH version 5.2.236) (Edgar 2010) at 97% similarity (min cluster size = 2 and de novo chimera checking). Reference sequences were obtained for each OTU. Reference sequences were further processed for chimeras using UCHIME (Edgar et al. 2011) against the Silva 119 database (Pruesse et al. 2007).

Taxonomic assignments for the 16S and 18S rRNA genes were made for the reference sequences using the blast (Altschul et al. 1990) algorithm in QIIME (evalue $1e^{-5}$) against the Silva 119 database. The eukaryotic component was functionally split into phytoplankton and heterotrophs (due to the sampling methods being unable to representatively sample metazoans these were removed from the analysis). OTU tables were constructed in QIIME and OTUs which only appeared in a single sample, were removed from further analysis. Samples were rarefied multiple times ($n = 100$) to an even depth of 5000 reads per sample and averaged reads per OTU were obtained. Samples not meeting the read threshold criteria were not incorporated into further analysis. To assess diversity the two replicate treatments were averaged. Reference sequences were aligned against the Silva 119 database using muscle (Edgar 2004) incorporated in the align_seqs.py script in QIIME. The similarity in the distribution of OTUs across the three experimental treatments was analyzed using venn.diagram in R (R development core team 2014). The R package *phyloseq* (McMurdie and Holmes 2013) was used to produce weighted and unweighted UniFrac distance matrices (Lozupone and Knight 2005) while generalized UniFrac distance matrices ($\alpha = 0.5$) were calculated with the package *GUniFrac* (Chen et al. 2012) based on the OTU table and phylogenetic tree constructed in QIIME. Non-metric multidimensional scaling (NMDS) plots were plotted in R using phyloseq and statistical analysis of the distance matrices was undertaken using Analysis of Similarity (ANOSIM) in *vegan* (Oksanen et al. 2013). Network analysis was undertaken based on Spearman's correlations calculated using rcorr (*Hmisc* package (Harrell 2014). Correlations were considered robust if Spearman's correlation coefficient (ρ) was both > 0.6 (or < -0.6 for negative correlations) and statistically significant ($p < 0.05$) (Barberán et al. 2012). p values were corrected for the false discovery rate in multiple comparisons using the Benjamini–Hochberg equation (Benjamini and Hochberg 1995). Networks were visualized using the igraph package in R. Mixing patterns in the networks were assessed using the assortativity.nominal function in igraph (Csárdi and Nepusz 2006) based on the equations of Newman (2003).

Results

Environmental variables

The evolution of temperature, salinity, and fluorescence during the experiment is presented in Supporting Information

Fig. S1. Salinity was shown to increase, throughout the experiment, possibly due to evaporation from the semi enclosed bags. Temperature dipped to 23°C during the second week before increasing again to around 27°C. Flow cytometry showed that no increase in the number of photosynthetic eukaryotes was observed in the control during the experiment (Supporting Information Fig. S2). Small increases in the abundance of nanoeukaryotes were observed in the nutrient treatments except for NPSc where a large increase around day 7 was observed followed by a rapid decline (Supporting Information Fig. S2b). Total bacteria counts increased during the experiment in all treatments (Supporting Information Fig. S2c). Increases in *Synechococcus* abundance was observed at the beginning of the experiment in both addition experiments but especially the NPSc treatment (Supporting Information Fig. S2d). The evolution of nutrients concentration is shown in Supporting Information Fig. S3. Elevated levels of silicate were observed in the bags with silicate addition remaining high throughout the experiment even when supplements were stopped (after day 14) (Supporting Information Fig. S3a). The NPc treatment showed increased levels of nitrate (Supporting Information Fig. S3b) and phosphate (Supporting Information Fig. S3d) until additions were stopped at the end of the second week while in the NPSc treatment declines were observed after a week before a second peak was observed 2 weeks into the experiment. In general both nitrite (Supporting Information Fig. S3c) and ammonia (Supporting Information Fig. S3e) increased throughout the experiment in all treatments including the control.

Sequence results

The 18S rRNA samples were part of a larger dataset containing 3,820,841 reads. After pre-filtering and OTU clustering, 24 OTUs were removed due to chimera checking against the SILVA 18S rRNA database. Subsequent to the removal of metazoan OTUs the eukaryotic fraction was rarefied multiple times ($n = 100$) to an even depth of 5000 reads per sampling point. The eukaryotes were then split into two functional groups (autotrophs and heterotrophs) resulting in a total of 442 eukaryotic phytoplankton OTUs and 687 OTUs representing microzooplankton.

For the prokaryotic fraction the whole dataset had a total of 4,641,251 reads which were sequenced and after quality filtering, 585 chimeras were removed when run against the SILVA 16S rRNA database. As with the eukaryotic fraction the prokaryotes were rarefied to 5000 reads per sampling point resulting in a total of 1407 OTUs for the presented treatments.

The majority of OTUs were observed in all treatments with 80% of prokaryotic OTUs shared between the three experimental setups. For the eukaryotic component substantial proportions of OTUs were only found in the nutrient enrichments (17.6% for heterotrophs and 30.0% for autotrophs).

Composition

Dinoflagellates dominated the photosynthetic component when the mesocosms were not supplemented with silicate (Fig. 1a,b) while the addition of silicate led to an increase in the proportion of reads attributed to diatoms (Fig. 1c). In the NPc treatment Chlorophyta (Chlorodenrales) reached a peak of 54.9% on day 14 (Fig. 1c).

Dinoflagellates were substantial components in all treatments with the genus *Amphidinium* being the major component at the beginning of the experiment. The high proportion of reads attributed to this group in the control accounted for the high dominance levels observed up to day 8 (Supporting Information Fig. S4a). In the control *Amphidinium* was succeeded by *Suessiaceae* and *Gonyaulacales* while in the NPc treatment *Kareniaceae* replaced *Amphidinium*.

Diatoms were prevalent in the NPSc reaching a peak proportion of 84.5%. A succession pattern in the NPSc treatment saw *Thalassiosira* being replaced by *Chaetoceros* before *Minutocellus* became the most dominant diatom genera. However by the time *Minutocellus* was the dominant diatom the proportion of diatoms in the phytoplankton had declined. In the NPc treatment *Thalassiosira* showed a small increase in the proportion of reads in the first 5 d.

Chrysophyceae (mainly Paraphysomonas) were the dominant component of the heterotrophic eukaryotes across all treatments (average 63.1%) (Fig. 1d–f). Picomonadea were present in all treatments, but particularly prevalent in the control (Fig. 1d). Other taxa, which were present in minor proportions (>2% on average across all treatments), were Intramacronucleata (9.5%), Syndinales (5.1%) and Ichthyosporea (2.6%). In all experimental treatments an increase in the level of dominance was observed between days 6–8.

In the prokaryotic fraction (Fig. 2) the three largest groups across the whole dataset were Rhodobacterales (25.5%), Flavobacteriales (23.0%) and subsection I of the Cyanobacteria (18.7%). An increase in the proportion of reads assigned to the autotrophic Cyanobacteria was observed in the first 10 d of both continuous treatments while in the control they were the dominant group in the last week of the experiment. This resulted in higher levels of dominance during these periods when cyanobacteria dominated (Supporting Information Fig. S4c).

Community structure

Significant differences were observed in the structure and composition of the eukaryotic communities (Fig. 3a–d). For the composition (weighted UniFrac) the autotrophs showed a larger effect (ANOSIM $R = 0.449$, $p = 0.001$ for autotrophs; $R = 0.186$, $p = 0.001$ for heterotrophs) while for the structure of the community (unweighted UniFrac) the opposite was observed (ANOSIM $R = 0.448$, $p = 0.001$ for autotrophs; $R = 0.488$, $p = 0.001$ for heterotrophs). For the bacterial component no significant difference was observed in both the structure and composition of the communities amongst the

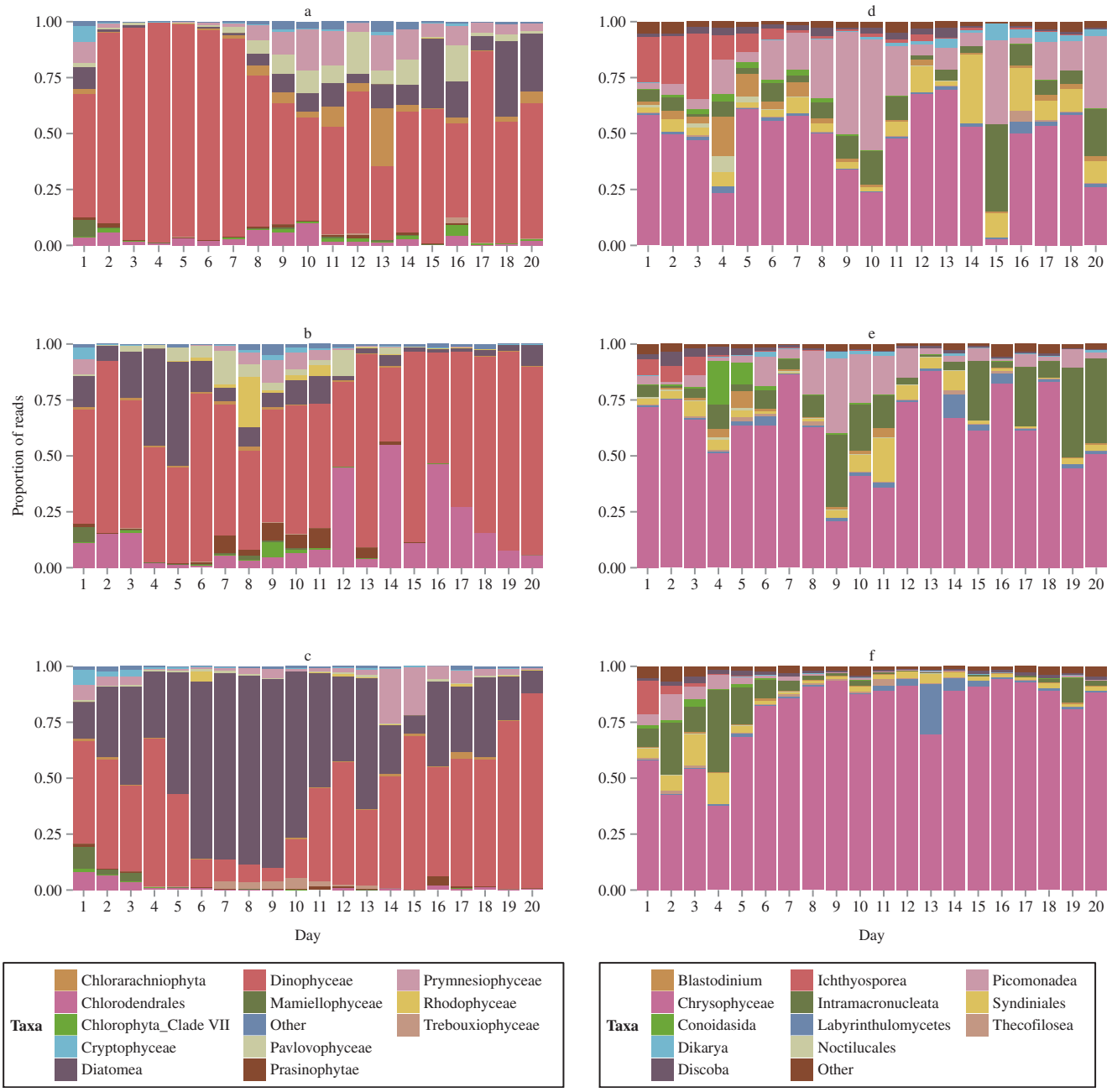

Fig. 1. Composition of eukaryotic phytoplankton and microzooplankton over the course of the mesocosm experiment: (**a**) phytoplankton in the control, (**b**) phytoplankton in the NPc, (**c**) phytoplankton in the NPSc, (**d**) microzooplankton in the control, (**e**) microzooplankton in the NPc, (**f**) microzooplankton in the NPSc. Others includes taxa which contributed less the 5% of the number of reads in a single sample.

different treatments (weighted UniFrac $R = 0.02$, $p = 0.189$; unweighted UniFrac $R = 0.023$, $p = 0.173$) as illustrated in Fig. 3e,f.

UniFrac dissimilarity plots showed that for both the eukaryotic autotrophs and heterotrophs there was a general trend for increase in dissimilarity between all treatments over the course of the experiment (Fig. 4a,b,d,e,g,h). However this was not a linear trend especially when abundance was taken into account (generalized and weighted UniFrac) where dissimilarity values for the autotrophs peaked early before declining (Fig. 4g). Microzooplankton in general showed a plateau in dissimilarity values during the last week of the experiment (Fig. 4h). For the bacterial component (Fig. 4c,f,i) a positive trend between the control and NPSc treatment was observed (Fig. 4f). Using unweighted UniFrac (which favors rare OTUs) microzooplankton

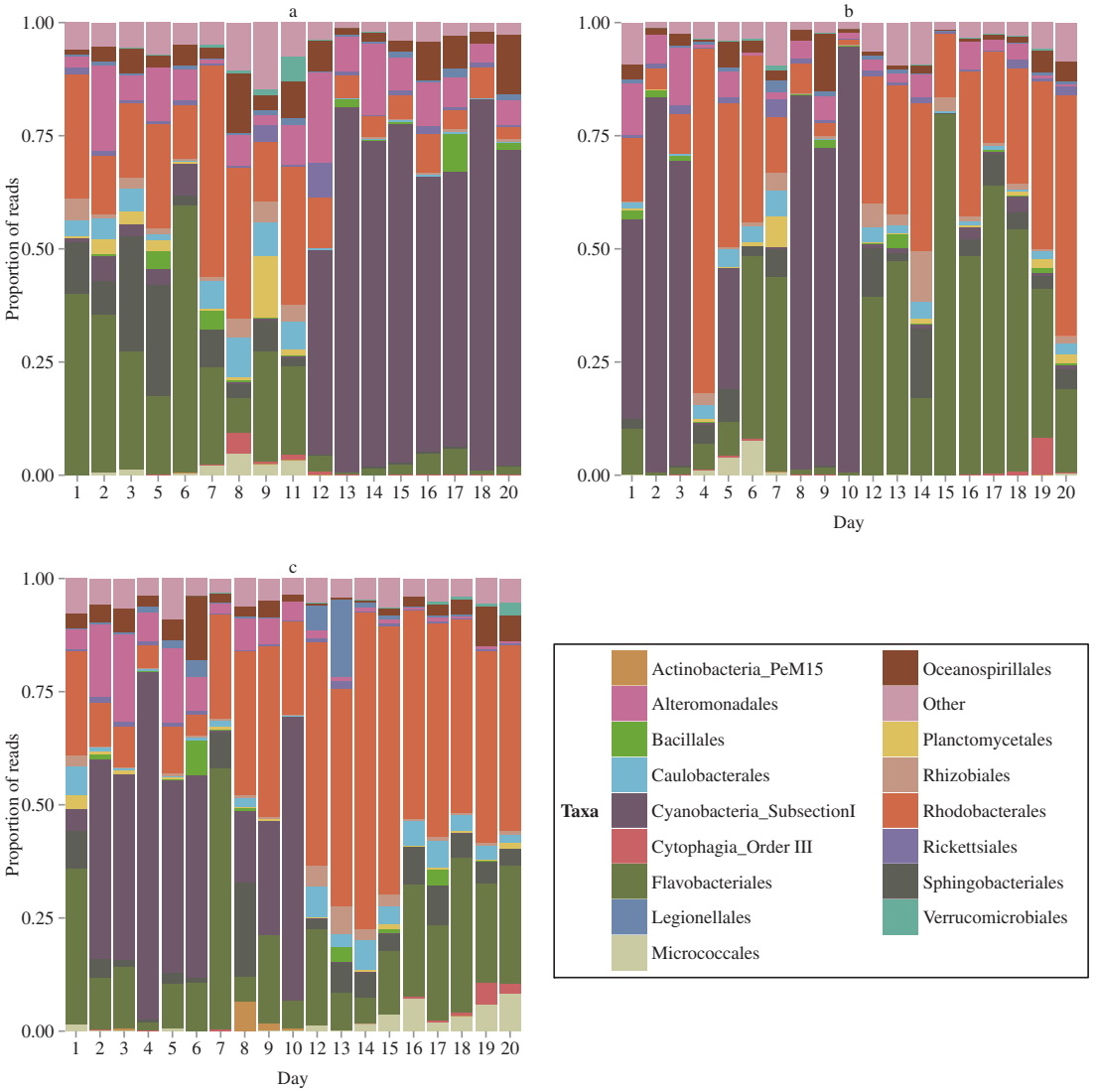

Fig. 2. Composition of the prokaryotic fraction during the course of the experiment in (**a**) the control, (**b**) NPc, and (**c**) NPSc. Others includes taxa which contributed less the 5% of the number of reads in a single sample. PeM15 is an uncultured order based on metagenomic sequence reads incorporated in the SILVA database.

responded to changes in the phytoplankton community in all comparisons while the prokaryotic community showed no response to the increase in dissimilarity in the phytoplankton community in the NPc-NPSc comparison (Fig. 5a,d,g). However, when using weighted UniFrac (which favors abundant OTUs) this trend is lost and there is no significant relationship in the trends (Fig. 5c,f,i). The generalized UniFrac algorithm shows a significant response of microzooplankton to the changes in the phytoplankton community but the prokaryotic response is not significant (Fig. 5b,e,h).

The response of the prokaryotic community to various environmental parameters was tested (chlorophyll *a*, nitrate, nitrite, phosphate and ammonia). The only significant correlation between the environmental parameters and dissimilarity was for ammonia in the C-NPSc dissimilarity comparison (Fig. 6a–i).

Network analysis

To assess the connections between abundant OTUs (classified as those averaging $>1\%$ in a treatment) within a treatment, Spearman correlations were calculated. Strong correlations were denoted by being statistically significant ($p<0.05$) and $\rho>0.6$ or <-0.6. The highest number of significant interactions were observed in the NPSc treatment (Fig. 7a–c).

Coexistence between OTUs, which were taxonomically related was higher than would be predicted if they were

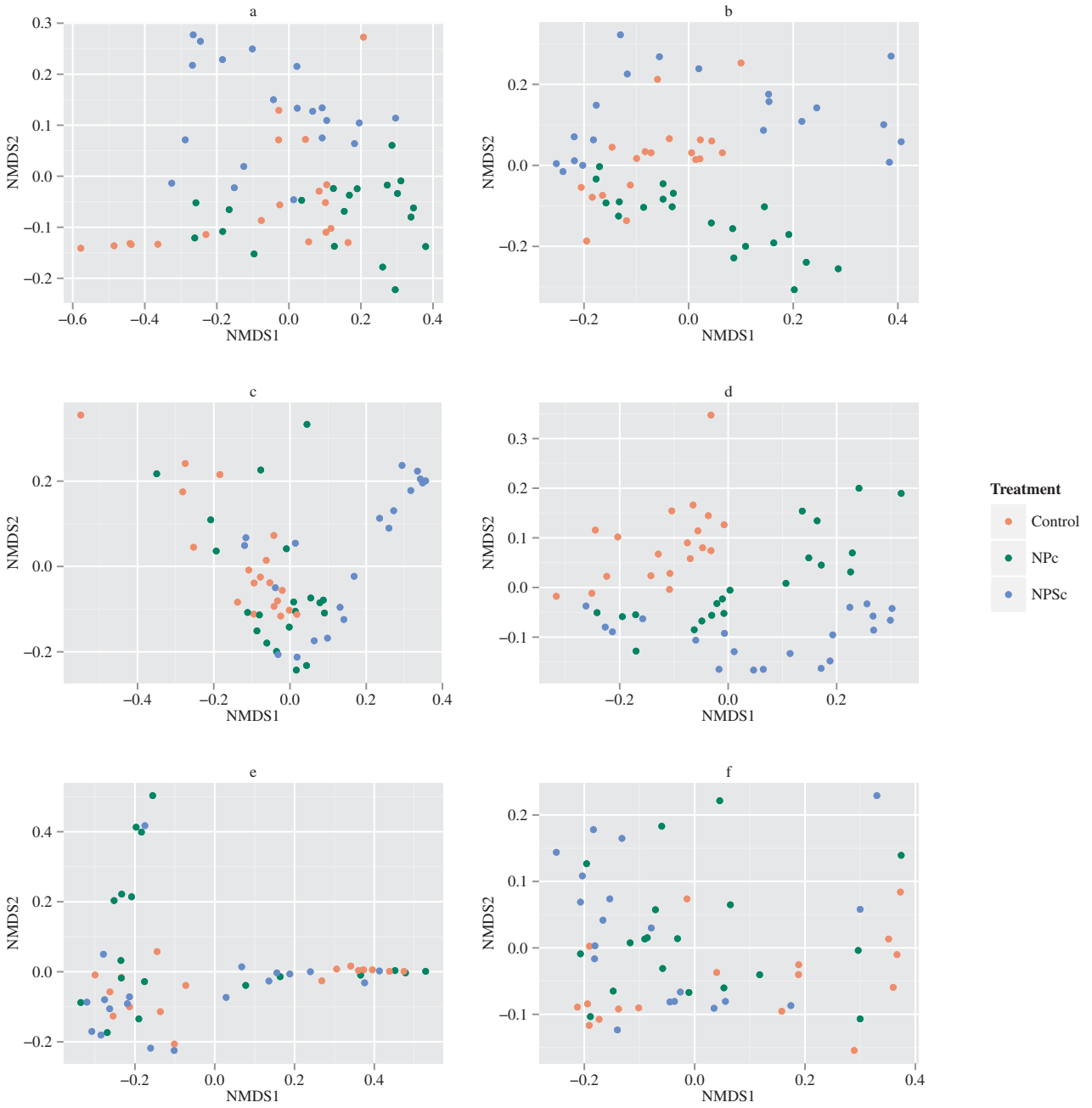

Fig. 3. NMDS plots based on UniFrac distance matrices for (**a**) weighted UniFrac of the phytoplankton, (**b**) unweighted UniFrac of the phytoplankton, (**c**) weighted UniFrac of the microzooplankton, (**d**) unweighted UniFrac of the microzooplankton, (**e**) weighted UniFrac of the prokaryotes, and (**f**) unweighted UniFrac of the prokaryotes.

randomly distributed especially in the NPc treatment (assortativity coefficient $r = 0.310$). This is exemplified by the majority of the top five strongest positive interactions in each treatment being between the same taxa (Table 1). In the NPSc treatment there were two OTUs (E148 and E170) related to the diatom genus *Chaetoceros* which formed part of the bloom. E148 is seen to increase in abundance during the course of the experiment while E170 declines (Supporting Information Fig. S5). A strong positive correlation between E170 and the most abundant Paraphysomonas OTU (E1302) is observed while the second most abundant Paraphysomonas OTU (E1666) has a negative relation due to its increase in abundance during the second half of the experiment.

The structure of the co-occurrences ($\rho > 0.6$ and $p < 0.05$) showed that OTUs were more likely to form edges with other OTUs belonging to the same taxa than would be randomly

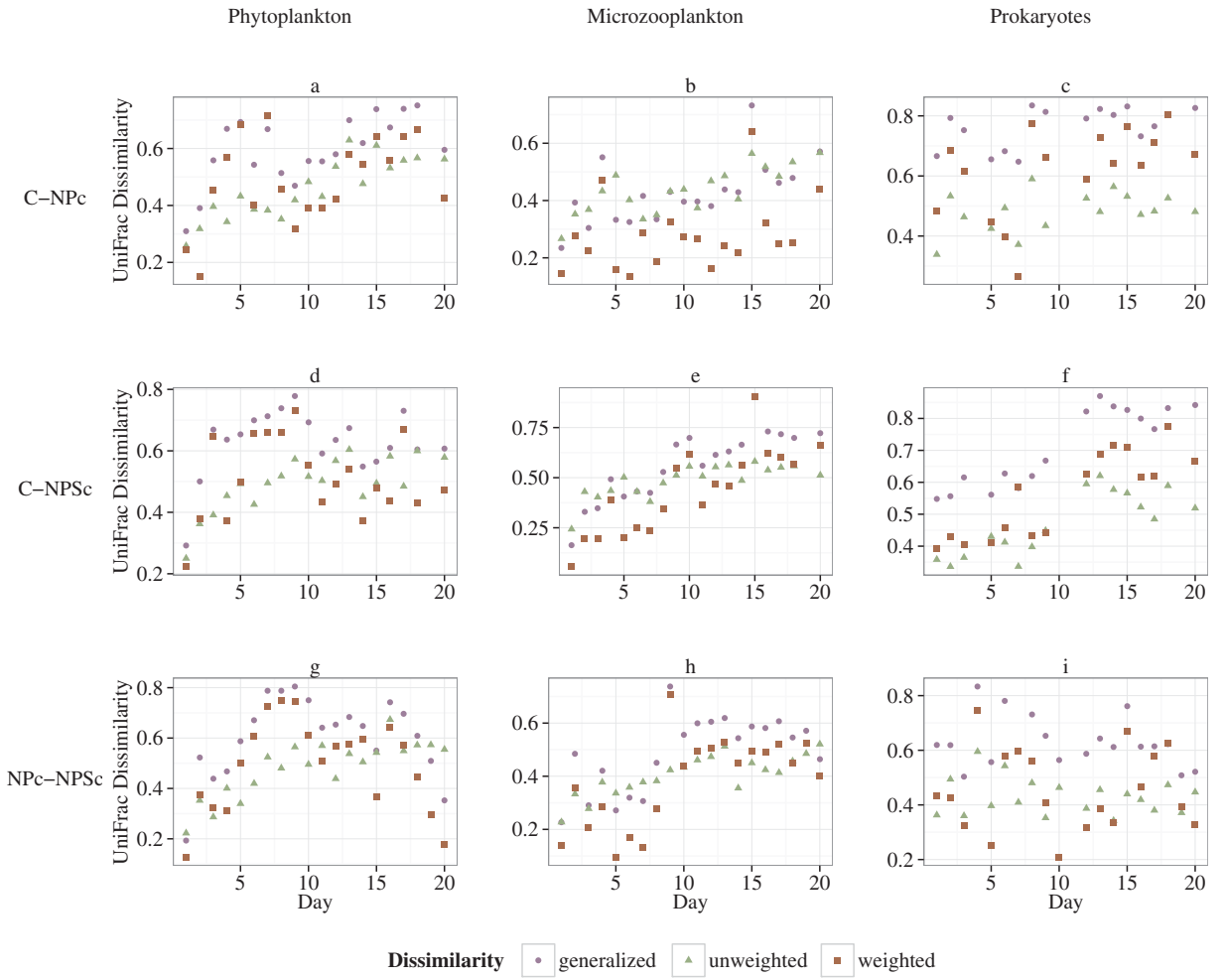

Fig. 4. Evolution in time of the unweighted, generalized and weighted Unifrac dissimilarities for phytoplankton, microzooplankton and prokaryotes amongst the three treatments. (**a**) C-NPc comparison for phytoplankton, (**b**) C-NPc comparison for microzooplankton, (**c**) C-NPc comparison for prokaryotes, (**d**) C-NPSc comparison for phytoplankton, (**e**) C-NPSc comparison for microzooplankton, (**f**) C-NPSc comparison for prokaryotes, (**g**) NPc-NPSc comparison for phytoplankton, (**h**) NPc-NPSc comparison for microzooplankton, (**i**) NPc-NPSc comparison for prokaryotes.

predicted with the NPc treatment showing the highest level of coexistence (assortativity coefficient $r = 0.3098$) while NPSc had the lowest coefficient ($r = 0.0492$).

The strongest interactions between groups showed that the bacterium Tenacibaculum was strongly correlated with OTUs of several phytoplankton including *Karlodinium* and *Amphidinium* while being negatively correlated with *Thalassiosira* in the NPc treatment (Table 2). In the NPSc treatment *Synechococcus a*nd Alteronomadaceae OTUs were strongly associated with OTUs from both *Chaetoceros* and *Amphidinium*. Bacteria–microzooplankton interactions showed Ichthyophonae having a strong association with several bacterial OTUs while Pezizomycotina had negative associations to similar bacterial taxa including Tropicibacter, Tenacibaculum and Saprospiraceae. In the NPSc treatment a range of Altermonadaceae OTUs were negatively correlated with a variety of Paraphysomonas OTUs. Phytoplankton–microzooplankton interactions showed that in the NPSc treatment *Chaetoceros* OTUs were positively correlated to several Paraphysomonas OTUs while negative associations were observed for *Amphidinium* and Paraphysomonas. In the NPc treatment negative correlations between several dinoflagellates were observed with Eugregarinorida.

Discussion

Bacteria and protists play a key role in the biogeochemical fluxes of the ocean (Azam et al. 1983; Azam 1998). However, the study of the main macroecological patterns and interactions in microbial communities has been limited by the limited taxonomic resolution in some of the groups. Further, research in different taxa has evolved in different directions and whereas molecular tools are nowadays widespread in the study of bacteria and archaea taxonomy, the work on large phytoplankton and microzooplankton is still mainly based

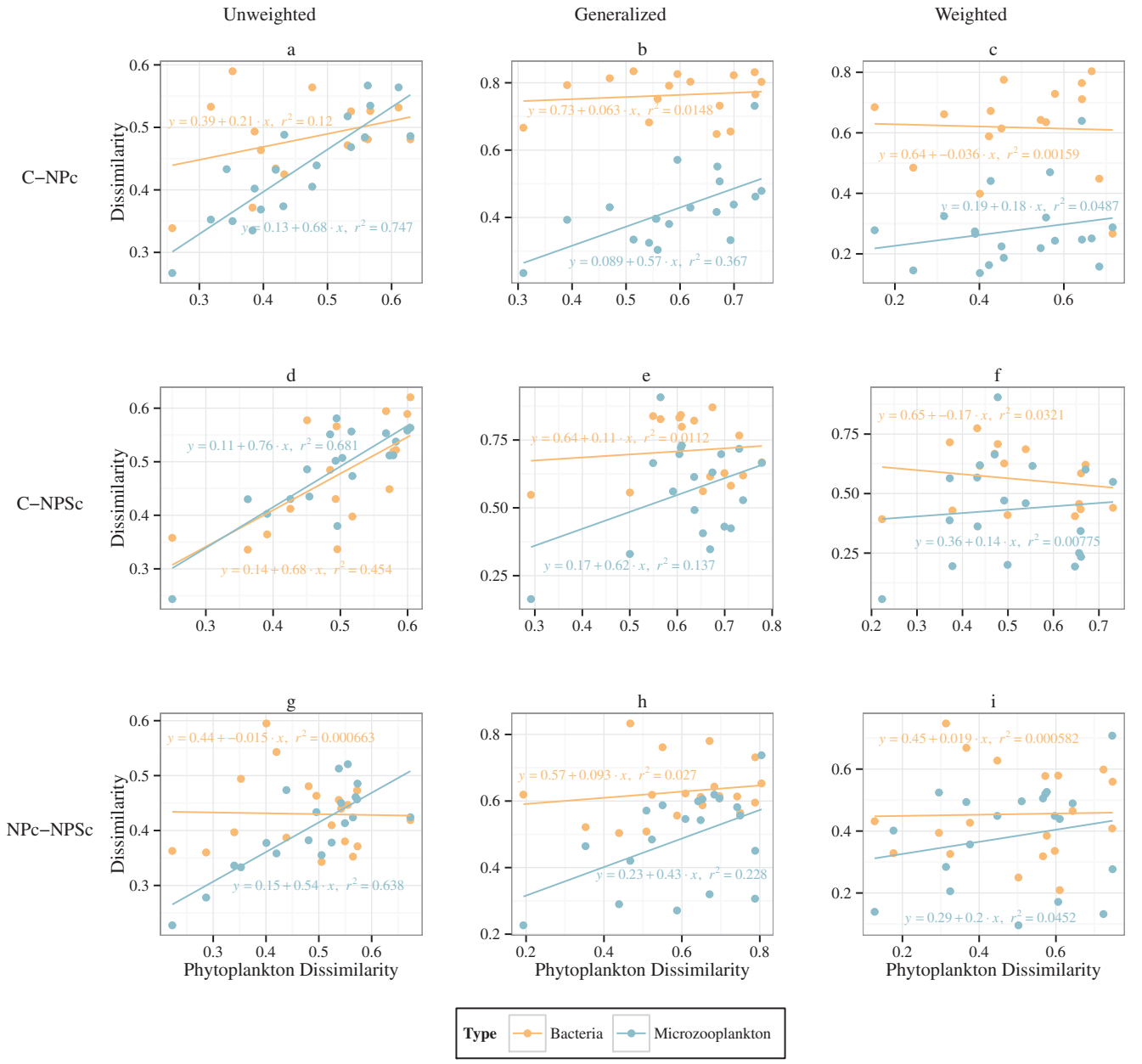

Fig. 5. Relation between the unweighted, generalized and weighted UniFrac dissimilarity of phytoplankton between treatments and the dissimilarity of bacteria and microzooplankton between the same treatments. (**a**) Unweighted C-NPc comparison, (**b**) generalized C-NPc comparison, (**c**) weighted C-NPc comparison, (**d**) unweighted C-NPSc comparison, (**e**) generalized C-NPSc comparison, (**f**) weighted C-NPSc comparison, (**g**) unweighted NPc-NPSc comparison, (**h**) generalized NPc-NPSc comparison, (**i**) weighted NPc-NPSc comparison.

on microscope analysis. However, molecular studies investigating the distribution of microbial eukaryotes in the environment are progressing (Bik et al. 2012) including studies in the marine environment (e.g., Cheung et al. 2010; Logares et al. 2012; Lie et al. 2014; de Vargas et al. 2015). Different methods of taxonomic classification are difficult to compare as DNA similarities close to the concept of species (e.g., 97%) often result in many more OTUs than the morphologically observed species (e.g., Orsini et al. 2004). As a consequence it is difficult to test whether major ecological theories, such as the relation between predator and prey biodiversity (Ehrlich and Raven 1964), also apply in the microbial loop. Although increasingly popular, there are inherent limitations in using molecular methods for such analysis. In particular, the limitation of existing reference databases for the taxa involved in the microbial loop make it difficult to assign an accurate low level taxonomy. Although dealing with unicellular organisms, it is also not obvious how the

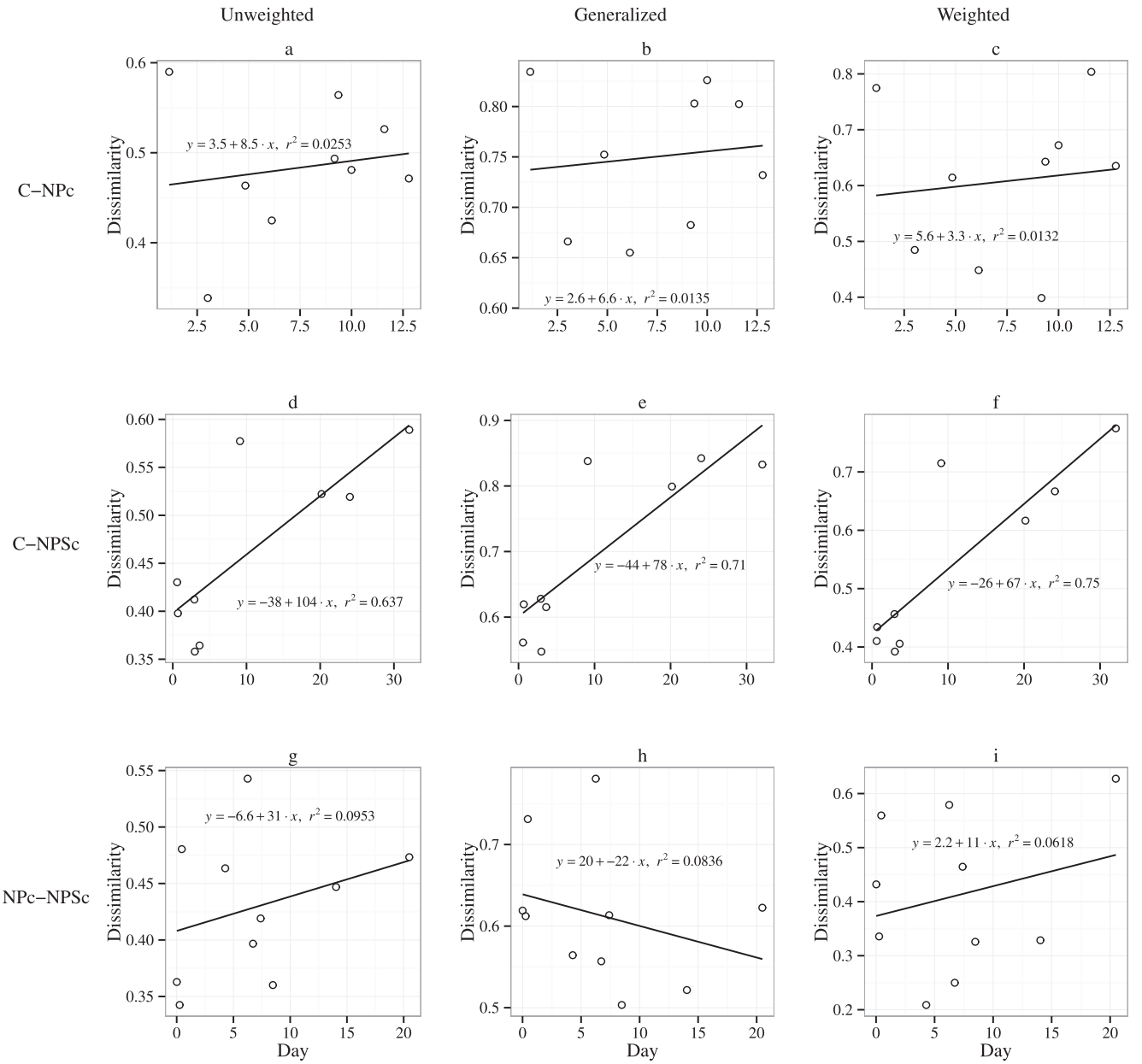

Fig. 6. Regression analysis comparing the change in ammonia concentrations between the treatments and unweighted, generalized and weighted UniFrac dissimilarities. (**a**) Unweighted C-NPc comparison, (**b**) generalized C-NPc comparison, (**c**) weighted C-NPc comparison, (**d**) unweighted C-NPSc comparison, (**e**) generalized C-NPSc comparison, (**f**) weighted C-NPSc comparison, (**g**) unweighted NPc-NPSc comparison, (**h**) generalized NPc-NPSc comparison, (**i**) weighted NPc-NPSc comparison.

number of reads translate into numbers of organisms. However, molecular methods allow the use of a coherent taxonomic classification (e.g., 97% similarity OTUs) across phylum as diverse as archaea, bacteria and different protists.

The use of such a common metric in our mesocosm study, where conditions more accurately replicate nature than laboratory microcosms resulted in two interesting and partially unexpected results. First, the microzooplankton community structure responds to alterations in the taxonomic composition of the phytoplankton community. Second, the bacterial community structure does not respond to changes in the phytoplankton community taxonomic composition (Fig. 5).

The phytoplankton community was shown to respond to the input of nutrients with a general increase in dissimilarity with time. However, in the comparison between the two nutrient enrichments (Fig. 4g) a decline in dissimilarity was noticed at the end of the experiment (especially with weighted UniFrac), which corresponded to the decline of the diatom

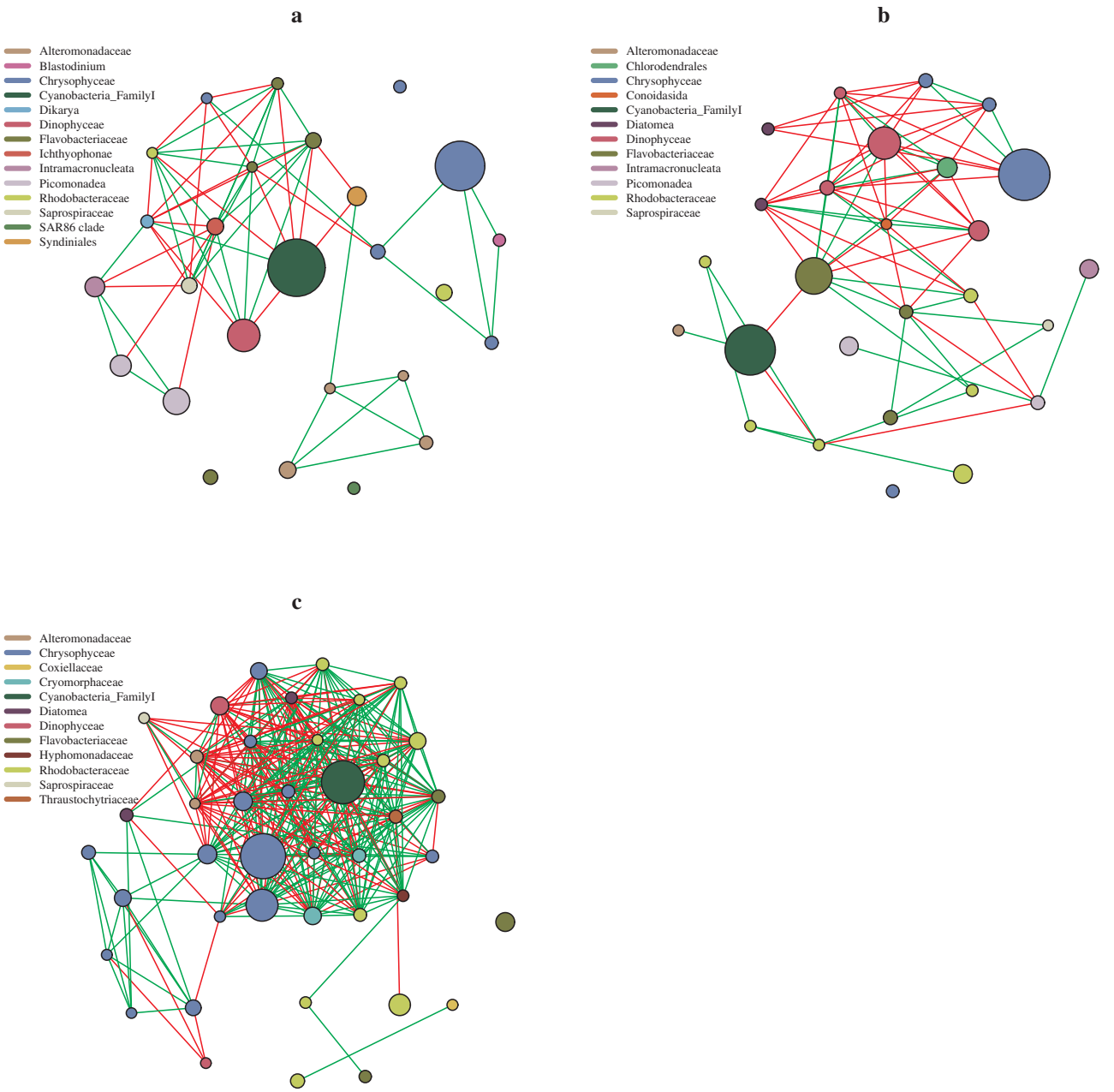

Fig. 7. Network analysis of the dominant OTUs (>1% of reads in a treatment) in (**a**) control, (**b**) NPc and (**c**) NPSc. Red edges denote a strong negative correlation ($\rho < -0.6$) while green edges characterize a strong positive correlation ($\rho > 0.6$). Size of the point corresponds to the proportional abundance of each OTU.

bloom in the NPSc treatment and the reemergence of dinoflagellates as the major component of the phytoplankton community. In the current experiment, contrary to what was discussed by Irigoien et al. (2004), but as suggested by Dolan (2005) the microzooplankton community changed with the composition of the phytoplankton community. A clear example of this was the switch in dominance of Paraphysomonas OTUs with the change in the type of dominant diatom (Supporting Information Fig. S5). The differences observed in the relation of the weighted and unweighted Unifrac dissimilarities between different trophic levels (bacteria vs. phytoplankton and phytoplankton vs. microzooplankton, Fig. 5) may explain the lack of correlation between microzooplankton and phytoplankton biodiversity observed previously (Irigoien et al. 2004). The unweighted Unifrac, which does not take into account abundance and therefore increases the influence of rare taxa, shows a good correlation between microzooplankton and phytoplankton dissimilarity in all treatments (Fig. 5a,d,g).

Table 1. The five most significant positive and negative interactions (including spearman's *r* value) for each treatment.

	Control			NPc			NPSc		
	Taxa	**Taxa**	***r***	**Taxa**	**Taxa**	***r***	**Taxa**	**Taxa**	***r***
Positive	Alteromonadaceae	Alteromonadaceae	0.971	Paraphysomonas	*Paraphysomonas*	0.988	*Owenweeksia*	*Owenweeksia*	0.97
	Paraphysomonas	Paraphysomonas	0.944	Paraphysomonas	Paraphysomonas	0.961	Roseibacterium	*Salinihabitans*	0.968
	Paraphysomonas	Paraphysomonas	0.941	Paraphysomonas	Paraphysomonas	0.949	Paraphysomonas	Paraphysomonas	0.961
	Alteromonadaceae	Alteromonadaceae	0.936	*Tetraselmis*	*Fragilidium*	0.934	Paraphysomonas	Paraphysomonas	0.956
	Paraphysomonas	Paraphysomonas	0.926	*Karlodinium*	*Fragilidium*	0.874	Paraphysomonas	Paraphysomonas	0.955
Negative	*Synechococcus*	*Tropicibacter*	−0.782	*Tenacibaculum*	Eugregarinorida	−0.817	Paraphysomonas	Paraphysomonas	−0.885
	Pezizomycotina	*Tropicibacter*	−0.808	*Karlodinium*	*Thalassiosira*	−0.822	*Synechococcus*	*Octadecabacter*	−0.889
	Ichthyophonae	Pezizomycotina	−0.814	*Fragilidium*	Eugregarinorida	−0.83	*Synechococcus*	Rhodobacteraceae	−0.898
	Pezizomycotina	*Tenacibaculum*	−0.851	*Karlodinium*	Eugregarinorida	−0.847	*Synechococcus*	Rhodobacteraceae	−0.9
	Amphidinium	Pezizomycotina	−0.852	*Tetraselmis*	Eugregarinorida	−0.865	Paraphysomonas	Alteromonadaceae	−0.911

This suggests that there can be grazing specialization in microzooplankton (John and Davidson 2001; Dolan et al. 2002) or specific deleterious effects (Turner 2006) contributing to shape the community species composition. However, when we use the generalized UniFrac (Fig. 5b,e,h) and more especially the weighted UniFrac (Fig. 5c,f,i), where abundance is taken into account and the influence of the most abundant species is higher, the correlation declines for the generalized UniFrac and is non significant for the weighted UniFrac. This suggests that, although specialist microzooplankton species populations developed in answer to the phytoplankton composition, those species did not reach sufficient abundances as to dominate the community and influence the weighted UniFrac. The lack of global correlation between phytoplankton and microzooplankton biodiversity may be due to different reasons. As suggested by Dolan (2005) it could be due to lack of taxonomic resolution, however in our data, where taxonomy is resolved at the same level (97% similarity) we do not observe correlation in biodiversity. Furthermore, microzooplankton not only consume phytoplankton, but also bacteria and other heterotrophic eukaryotes, thus the diversity of the phytoplankton may not be the best indicator. Finally, the fact that the microzooplankton community changes with the phytoplankton one does not imply that there should be a correlation in the biodiversity.

Unlike the microzooplankton community, we observe that there are no changes in dissimilarity in the bacterial community between mesocosms dominated by diatoms and those dominated by dinoflagellates. In fact, we observe a significant correlation between the dissimilarity of phytoplankton and microzooplankton in the NPc and NPSc treatments but not between bacterial and phytoplankton dissimilarities. However, we observe that dissimilarity increases in the bacterial communities between the control and the nutrient treatments where phytoplankton biomass and subsequently dissolved organic matter would be increased. Bacterial communities do change during a phytoplankton bloom, however whether the changes are due to species succession, increases in biomass or viral infections is difficult to evaluate (Riemann et al. 2000). Phytoplankton, have previously been shown to have different associated bacteria (Grossart et al. 2005) and laboratory microcosm experiments, using turbulence to favor growth of different phytoplankton, have resulted in differentiated bacterial communities (Pinhassi et al. 2004). These results suggest that the bacterial community should show a response to blooms dominated by different groups, however such an effect was not observed in this experiment. This may be due to the prokaryotic community composition being driven by stronger factors than phytoplankton species composition. High differences in the concentration of ammonia between the control and NPSc treatments had a significant correlation with the dissimilarity between the communities (Fig. 6) and it could be suggested that the recycling of ammonia was the predominant

Table 2. The five most significant positive and negative interactions (including spearman's *r* values) for each treatment between groups (prokaryotes, phytoplankton and microzooplankton).

Bacteria-phytoplankton

Control			NPc			NPSc		
Taxa	**Taxa**	***r***	**Taxa**	**Taxa**	***r***	**Taxa**	**Taxa**	***r***
Tenacibaculum	*Amphidinium*	0.772	*Tenacibaculum*	*Karlodinium*	0.753	*Synechococcus*	*Amphidinium*	0.862
Polaribacter	*Amphidinium*	0.745	*Tenacibaculum*	*Amphidinium*	0.712	*Synechococcus*	*Chaetoceros*	0.808
Tropicibacter	*Amphidinium*	0.639	*Tenacibaculum*	*Tetraselmis*	0.701	Alteromonadaceae	*Amphidinium*	0.805
			Tenacibaculum	*Fragilidium*	0.626	Alteromonadaceae	*Chaetoceros*	0.736
			Thalassobius	*Amphidinium*	0.622	Alteromonadaceae	*Amphidinium*	0.719
			Formosa	*Amphidinium*	−0.643	Rhodobacteraceae	*Amphidinium*	−0.799
			Thalassobius	*Thalassiosira*	−0.647	*Owenweeksia*	*Chaetoceros*	−0.812
			Formosa	*Thalassiosira*	−0.648	Flavobacteriaceae	*Amphidinium*	−0.816
			Tenacibaculum	*Thalassiosira*	−0.724	*Gaetbulicola*	*Amphidinium*	−0.837
			Tenacibaculum	*Amphidinium*	−0.765	*Octadecabacter*	*Amphidinium*	−0.844

Bacteria-microzooplankton

Control			NPc			NPSc		
Taxa	**Taxa**	***r***	**Taxa**	**Taxa**	***r***	**Taxa**	**Taxa**	***r***
Tropicibacter	Ichthyophonae	0.833				*Octadecabacter*	Paraphysomonas	0.907
Saprospiraceae	Syndiniales I	0.777				*Roseibacterium*	Paraphysomonas	0.874
Tenacibaculum	Ichthyophonae	0.689				*Octadecabacter*	Paraphysomonas	0.870
Formosa	Ichthyophonae	0.684				*Gaetbulicola*	Paraphysomonas	0.846
Saprospiraceae	Ichthyophonae	0.681				*Octadecabacter*	Paraphysomonas	0.842
Saprospiraceae	Pezizomycotina	−0.742	*Formosa*	Picomonadea	−0.612	Alteromonadaceae	Paraphysomonas	−0.840
Tenacibaculum	Paraphysomonas	−0.748	*Thalassobius*	Eugregarinorida	−0.619	Alteromonadaceae	Paraphysomonas	−0.864
Polaribacter	Pezizomycotina	−0.758	*Thalassobius*	Picomonadea	−0.686	Alteromonadaceae	Paraphysomonas	−0.870
Tropicibacter	Pezizomycotina	−0.808	*Formosa*	Eugregarinorida	−0.703	Alteromonadaceae	Paraphysomonas	−0.879
Tenacibaculum	Pezizomycotina	−0.851	*Tenacibaculum*	Eugregarinorida	−0.817	Alteromonadaceae	Paraphysomonas	−0.911

Phytoplankton-microzooplankton

Control			NPc			NPSc		
Taxa	**Taxa**	***r***	**Taxa**	**Taxa**	***r***	**Taxa**	**Taxa**	***r***
Amphidinium	Ichthyophonae	0.668	*Thalassiosira*	Eugregarinorida	0.871	*Chaetoceros*	Paraphysomonas	0.805
			Amphidinium	Eugregarinorida	0.809	*Chaetoceros*	Paraphysomonas	0.779
						Chaetoceros	Paraphysomonas	0.745
						Chaetoceros	Paraphysomonas	0.707
						Chaetoceros	Paraphysomonas	0.653
Amphidinium	Syndiniales I	−0.713	*Minutocellus*	Paraphysomonas	−0.753	*Amphidinium*	Paraphysomonas	−0.788
Amphidinium	Pezizomycotina	−0.852	*Amphidinium*	Eugregarinorida	−0.771	*Karlodinium*	Paraphysomonas	−0.818
			Fragilidium	Eugregarinorida	−0.830	*Amphidinium*	Paraphysomonas	−0.843
			Karlodinium	Eugregarinorida	−0.847	*Amphidinium*	Paraphysomonas	−0.867
			Tetraselmis	Eugregarinorida	−0.865	*Amphidinium*	Paraphysomonas	−0.870

driving force in bacterial community composition at the end of the experiment.

Previous studies have utilized network analysis based on molecular data to show correlations between taxa in the marine environment (Steele et al. 2011; Gilbert et al. 2012; Chow et al. 2013). In the current study, we observe some antagonistic effects such as between a variety of Rhodobacaterales OTUs and *Amphidinium* (a prebloom species) and the

diatom species that bloomed, *Chaetoceros* (Fig. 7). However, such effects are not widespread enough as to alter the community structure. Although the intracellular biochemical composition differs substantially between algal classes (Quigg et al. 2003), this result suggests that the same types of bacteria can utilize the excreted extracellular organic matter. Furthermore, it has to be considered that the composition of the organic matter excreted by a single species also varies with the growth phase of the population (Vidoudez and Pohnert 2012), which contributes to a complex chemical landscape during the bloom succession. Actually, in our experiment the bacterial community dissimilarity between different bags at time 0 is much higher than that of phytoplankton and microzooplankton, suggesting a much higher heterogeneity. Therefore, in absence of a direct toxic interactions between bacteria and phytoplankton (e.g., Paul and Pohnert 2011), our results indicate that the composition of the planktonic bacterial community might be more strongly related to the phase of the bloom than to the phytoplankton species dominating the bloom.

To summarize, the use of molecular tools allows sufficient taxonomic resolution to follow the changes of the microzooplankton and bacterial communities during blooms of different phytoplankton groups (diatoms and dinoflagellates). The microzooplankton community differentiates in relation to the phytoplankton composition, whereas the bacterial community differentiation is possibly more related to the increase in biomass/detritus and ammonia than to the differences in phytoplankton composition.

References

Altschul, S. F., W. Gish, W. Miller, E. W. Myers, and D. J. Lipman. 1990. Basic Local Alignment Search Tool. J. Mol. Biol. **215**: 403–410. doi:10.1016/S0022-2836(05)80360-2

Amaral-Zettler, L. A., E. A. McCliment, H. W. Ducklow, and S. M. Huse. 2009. A method for studying protistan diversity using massively parallel sequencing of V9 hypervariable regions of small-subunit ribosomal RNA genes. PloS ONE **4**: e6372–e6372. doi:10.1371/journal.pone.0006372

Azam, F. 1998. Microbial control of oceanic carbon flux: The plot thickens. Science **280**: 694–695. doi:10.1126/science.280.5364.694

Azam, F., T. Fenchel, J. G. Field, J. S. Gray, L. A. Meyer-Reil, and F. Thingstad.1983. The ecological role of water column microbes in the sea. Mar. Ecol. Prog. Ser. **10**: 257–263. doi:10.3354/meps010257

Barberán, A., S. T. Bates, E. O. Casamayor, and N. Fierer. 2012 Using network analysis to expore co-occurrence patterns in soil microbial communities. ISME J. **6**: 343–351. doi:10.1038/ismej.2011.119

Benjamini, Y., and Y. Hochberg. 1995. Controlling the false discovery rate: A practical and powerful approach to multiple testing. J. R. Stat. Soc. Ser. B **57**: 289–300. doi:10.2307/2346101

Bik, H. M., D. L. Porazinska, S. Creer, J. G. Caporaso, R. Knight, and W. K. Thomas. 2012. Sequencing our way towards understanding global eukaryotic biodiversity. Trends Ecol. Evol. **27**: 233–243. doi:10.1016/j.tree.2011.11.010

Billett, D. S. M., R. S. Lampitt, and R. F. C. Mantoura. 1983. Seasonal sedimentation of phytoplankton to the deep-sea benthos. Nature **302**: 520–522. doi:10.1038/302520a0

Brügmann, L., and K. Kremling. 2007. Sampling, p. 1–24. *In* K. Grasshoff, K. Kremling and M. Ehrhardt [eds.], Methods of seawater analysis. WILEY-VCH Verlag.

Buchan, A., G. R. LeCleir, C. A. Gulvik, and J. M. González. 2014. Master recyclers: Features and functions of bacteria associated with phytoplankton blooms. Nat. Rev. Microbiol. **12**: 686–698. doi:10.1038/nrmicro3326

Caporaso, J. G. K., and others. 2010. QIIME allows analysis of highthroughput community sequencing data. Nat. Methods **7**: 335–336. doi:10.1038/nmeth.f.303

Caron, D. A., P. D. Countway, and M. V. Brown. 2004. The growing contributions of molecular biology and immunology to protistan ecology: Molecular signatures as ecological tools. J. Eukaryot. Microbiol. **51**: 38–48. doi:10.1111/j.1550-7408.2004.tb00159.x

Chen, J., and others. 2012. Associating microbiome composition with environmental covariates using generalized UniFrac distances. Bioinformatics **28**: 2106–2113. doi:10.1093/bioinformatics/bts342

Cheung, M. K., C. H. Au, K. H. Chu, H. S. Kwan, and C. K. Wong. 2010. Composition and genetic diversity of picoeukaryotes in subtropical coastal waters as revealed by 454 pyrosequencing. ISME J. **4**: 1053–1059. doi:10.1038/ismej.2010.26

Chow, C. E., and others. 2013. Temporal variability and coherence of euphotic zone bacterial communities over a decade in the Southern California Bight. ISME J. **7**: 2259–2273. doi:10.1038/ismej.2013.122

Cole, J. J., S. Findlay, and M. L. Pace. 1988. Bacterial production in fresh and saltwater ecosystems—a system overview. Mar. Ecol. Prog. Ser. **43**: 1–10. doi:10.3354/meps043001

Csárdi, G., and T. Nepusz. 2006. The igraph software package for complex network research. InterJournal Complex Systems, **1695**.

de Vargas, C., and others. 2015. Eukaryotic plankton diversity in the sunlit ocean. Science **348**. doi:10.1126/science.1261605

Dolan, J. R. 2005. Marine ecology—different measures of biodiversity. Nature **433**: E9. doi:10.1038/nature03320

Dolan, J. R., H. Claustre, F. Carlotti, S. Plounevez, and T. Moutin. 2002. Microzooplankton diversity: Relationships of tintinnid ciliates with resources, competitors and predators from the Atlantic Coast of Morocco to the Eastern

Mediterranean. Deep-Sea Res. Part I Oceanogr. Res. Pap. **49**: 1217–1232. doi:10.1016/S0967-0637(02)00021-3

Ducklow, H. W., D. L. Kirchman, H. L. Quinby, C. A. Carlson, and H. G. Dam. 1993. Stocks and dynamics of bacterioplankton carbon during the spring bloom in the eastern north-Atlantic Ocean. Deep-Sea Res. Part II Top. Stud. Oceanogr. **40**: 245–263. doi:10.1016/0967-0645(93)90016-G

Edgar, R. C. 2004. MUSCLE: Multiple sequence alignment with high accuracy and high throughput. Nucleic Acids Res. **32**: 1792–1797. doi:10.1093/nar/gkh340

Edgar, R. C. 2010. Search and clustering orders of magnitude faster than BLAST. Bioinformatics **26**: 2460–2461. doi:10.1093/bioinformatics/btq461

Edgar, R. C., B. J. Haas, J. C. Clemente, C. Quince, and R. Knight. 2011. UCHIME improves sensitivity and speed of chimera detection. Bioinformatics **27**: 2194–2200. doi:10.1093/bioinformatics/btr381

Ehrlich, P. R., and P. H. Raven. 1964. Butterflies and plants: A study in coevolution. Evolution **18**: 586–608. doi:10.2307/2406212

Gilbert, J. A., and others. 2012. Defining seasonal marine microbial community dynamics. ISME J. **6**: 298–308. doi:10.1038/ismej.2011.107

Grasshoff, K., M. Ehrhardt, and K. Kremling (eds.). 1983. Methods of seawater analysis, p. 419. Verlag Chemie.

Grossart, H. P., F. Levold, M. Allgaier, M. Simon, and T. Brinkhoff. 2005. Marine diatom species harbour distinct bacterial communities. Environ. Microbiol. **7**: 860–873. doi:10.1111/j.1462-2920.2005.00759.x

Harrell, F. E. 2014 Hmisc: Harrell Miscellaneous. R package version 3.16-0. http://CRAN.R-project.org/package=Hmisc.

Irigoien, X., R. P. Harris, R. N. Head, D. Cummings, B. Harbour, and B. Myer-Harms. 2000. Feeding selectivity and egg production of *Calanus helgolandicus* in the English Channel. Limnol. Oceanogr. **45**: 44–54. doi:10.4319/lo.2000.45.1.0044

Irigoien, X., J. Huisman, and R. P. Harris. 2004. Global biodiversity patterns of marine phytoplankton and zooplankton. Nature **429**: 863–867. doi:10.1038/nature02593

John, E. H., and K. Davidson. 2001. Prey selectivity and the influence of prey carbon: nitrogen ratio on microflagellate grazing. J. Exp. Mar. Biol. Ecol. **260**: 93–111. doi:10.1016/S0022-0981(01)00244-1

Klindworth, A., E. Pruesse, T. Schweer, J. Peplies, C. Quast, M. Horn, and F. O. Glöckner. 2013. Evaluation of general 16S ribosomal RNA gene PCR primers for classical and next-generation sequencing-based diversity studies. Nucleic Acids Res. **41**: e1. doi:10.1093/nar/gks808

Kremling, K., and L. Brügmann. 2007. Filtration and storeage, p. 1–24. *In* K. Grasshoff, K. Kremling and M. Ehrhardt [eds.], Methods of seawater analysis, 3rd ed. Verlag GmbH.

Li, W., and A. Godzik. 2006. Cd-hit: A fast program for clustering and comparing large sets of protein or nucleotide sequences. Bioinformatics **22**: 1658–1659. doi:10.1093/bioinformatics/btl158

Lie, A. A., and others. 2014. Investigating microbial eukaryotic diversity from a global census: Insights from a comparison of pyrotag and full-length sequences of 18S rRNA genes. Appl. Environ. Microbiol. **80**: 4363–4373. doi:10.1128/AEM.00057-14

Löder, M. G. J., C. Meunier, K. H. Wiltshire, M. Boersma, and N. Aberle. 2011. The role of ciliates, heterotrophic dinoflagellates and copepods in structuring spring plankton communities at Helgoland Roads, North Sea. Mar. Biol. **158**: 1551–1580. doi:10.1007/s00227-011-1670-2

Logares, R., S. Audic, S. Santini, M. C. Pernice, C. de Vargas, and R. Massana. 2012. Diversity patterns and activity of uncultured marine heterotrophic flagellates unveiled with pyrosequencing. ISME J. **6**: 1823–1833. doi:10.1038/ismej.2012.36

Longhurst, A. R., and W. G. Harrison. 1989. The biological pump—profiles of plankton production and consumption in the upper ocean. Prog. Oceanogr. **22**: 47–123. doi:10.1016/0079-6611(89)90010-4

Lozupone, C., and R. Knight. 2005 UniFrac: A new phylogenetic method for comparing microbial communities. Appl. Environ. Microbiol. **71**: 8228–8235. doi:10.1128/AEM.71.12.8228-8235.2005

McMurdie, P. J., and S. Holmes. 2013. phyloseq: An R Package for reproducible interactive analysis and graphics of microbiome census data. PloS ONE **8**: e61217. doi:10.1371/journal.pone.0061217

Moran, X. A. G., M. Estrada, J. M. Gasol, and C. Pedros-Alio. 2002. Dissolved primary production and the strength of phytoplankton bacterioplankton coupling in contrasting marine regions. Microb. Ecol. **44**: 217–223. doi:10.1007/s00248-002-1026-z

Newman, M. E. J. 2003. Mixing patterns in networks. Phys. Rev. **E67**: 026126. doi:10.1103/PhysRevE.67.026126

Oksanen, J. F., and others. 2013 vegan: Community Ecology Package. R package version 2.0.10. Available from http://CRAN.R-project.org/package=vegan

Orsini, L., G. Procaccini, D. Sarno, and M. Montresor. 2004. Multiple rDNA ITS-types within the diatom *Pseudo-nitschia delicatissima* (Bacillariophyceae_ and their relative abundances across a spring bloom in the Gulf of Naples. Mar. Ecol. Prog. Ser. **271**: 87–98. doi:10.3354/meps271087

Paul, C., and G. Pohnert. 2011. Interactions of the algicidal bacterium *Kordia algicida* with diatoms: Regulated protease excretion for specific algal lysis. PloS ONE **6**: e21032. doi:10.1371/journal.pone.0021032

Pinhassi, J., and T. Berman. 2003. Differential growth response of colony-forming alpha- and gamma-proteobacteria in dilution culture and nutrient addition experiments from Lake Kinneret (Israel), the eastern Mediterranean Sea, and the Gulf of Eilat. Appl. Environ. Microbiol. **69**: 199–211. doi:10.1128/AEM.69.1.199-211.2003

Pinhassi, J., M. Montserrat Sala, H. Havskum, F. Peters, Ò. Guadayol, A. Malits, and C. Marrasé. 2004. Changes in bacterioplankton composition under different phytoplankton regimens. Appl. Environ. Microbiol. **70**: 6753–6766. doi:10.1128/AEM.70.11.6753-6766.2004

Pruesse, E., C. Quast, K. Knittel, B. M. Fuchs, W. Ludwig, J. Peplies, and F. O. Glöckner. 2007. SILVA: A comprehensive online resource for quality checked and aligned ribosomal RNA sequence data compatible with ARB. Nucleic Acids Res. **35**: 7188–7196. doi:10.1093/nar/gkm864

Quigg, A., and others. 2003. The evolutionary inheritance of elemental stoichiometry in marine phytoplankton. Nature **425**: 291–294. doi:10.1038/nature01953

R development core team. 2014. R: A language and environment for statistical computing. R Foundation for Statistical Computing, Vienna, Austria. ISBN 3-900051-07-0. Available from http://www.R-project.org

Riemann, L., G. F. Steward, and F. Azam. 2000. Dynamics of bacterial community composition and activity during a mesocosm diatom bloom. Appl. Environ. Microbiol. **66**: 578–587. doi:10.1128/AEM.66.2.578-587.2000

Rink, B., S. Seeberger, T. Martens, C.-D. Duerselen, M. Simon, and T. Brinkhoff. 2007. Effects of phytoplankton bloom in a coastal ecosystem on the composition of bacterial communities. Aquat. Microb. Ecol. **48**: 47–60. doi:10.3354/ame048047

Rose, J. M., and D. A. Caron. 2007. Does low temperature constrain the growth rates of heterotrophic protists? Evidence and implications for algal blooms in cold waters. Limnol. Oceanogr. **52**: 886–895. doi:10.4319/lo.2007.52.2.0886

Sherr, E. B., and B. F. Sherr. 2002. Significance of predation by protists in aquatic microbial food webs. Antonie Van Leeuwenhoek Int. J. Gen. Mol. Microbiol. **81**: 293–308. doi:10.1023/A:1020591307260

Steele, J. A., and others. 2011. Marine bacterial, archaeal and protistan association networks reveal ecological linkages. ISME J. **5**: 1414–1425. doi:10.1038/ismej.2011.24

Teeling, H., and others. 2012. Substrate-controlled succession of marine bacterioplankton populations induced by a phytoplankton bloom. Science **336**: 608–611. doi:10.1126/science.1218344

Turner, J. T. 2006. Harmful algae interactions with marine planktonic grazers, p. 259–270. *In* E. Granéli and J. T. Turner [eds.], Ecology of harmful algae. Springer.

Vidoudez, C., and G. Pohnert. 2012. Comparative metabolomics of the diatom *Skeletonema marinoi* in different growth phases. Metabolomics **8**: 654–669. doi:10.1007/s11306-011-0356-6

Wyman, M., J. T. Davies, D. W. Crawford, and D. A. Purdie. 2000. Molecular and physiological responses of two classes of marine chromophytic phytoplankton (Diatoms and Prymnesiophytes) during the development of nutrient-stimulated blooms. Appl. Environ. Microbiol. **66**: 2349–2357. doi:10.1128/AEM.66.6.2349-2357.2000

Acknowledgments

The authors would like to thank all those who helped during the sampling of the mesocosm experiment and especially Ioannis Georgakakis. Also the authors would like to thank Prof. Jean-Philippe Croué for allowing the flow cytometry samples to be analyzed using his equipment. Thanks are also given to the reviewers for their constructive comments during the review process. This research was supported by baseline funding provided by KAUST to Prof. Xabier Irigoien. The authors declare no conflicts of interest.

Submitted 2 March 2015
Revised 4 July 2015, 30 August 2015
Accepted 15 September 2015

Associate editor: Ian Hewson